Lattice Gas Automata and Pattern Formation, L. Lawniczak & R. Kapral, eds.
Fields Institute, Canada (1994)

New class of cellular automata for reaction-diffusion systems applied to the CIMA reaction

Jörg R. Weimar and Jean-Pierre Boon
Faculté des Sciences, C.P. 231
Université Libre de Bruxelles, B-1050 Bruxelles, Belgium
E-mail: jweimar@ulb.ac.be, jpboon@ulb.ac.be

May 22, 1993

Abstract

We present a class of cellular automata (CAs) for modelling reaction-diffusion systems. The construction of the CA is general enough to be applicable to a large class of reaction-diffusion equations. The automata are based on a running average procedure to implement diffusion, and on a probabilistic table-lookup to implement the reaction. As an example application we present the Brandeisator (Lengyl-Epstein model for the chlorite-iodide-malonic acid reaction CIMA), which exhibits a rich set of behaviors: oscillations, hexagonal structures, stripes, and spirals. We investigate cases showing mixed states, in which different structures coexist in space: isolated spots, isolated regions of hexagons in a surrounding homogeneous region, coexistence between stripes and oscillations, and hexagons and stripes. The cellular automaton approach has the following advantages: fast simulations of large systems, easy implementation of noise in the system, and connections to other, more phenomenologically constructed CAs.

1 Introduction

Cellular automata (CA)[17] have become a valuable method to investigate reaction-diffusion (R-D) systems[7]. Most models are based on a qualitative approach, and cannot be used for quantitative analyses of R-D systems [5, 4, 10, 13]. Other models are based on a singular perturbation analysis and are only valid in a certain limit[15, 16]. This is the main reason why some experimentalists and researchers working with partial differential equations do not view CAs as a useful tool. In this paper we present a new class of CAs which is suitable for modelling many reaction-diffusion systems in a quantitatively correct way. The new CAs are operationally more efficient and more versatile than the reactive lattice gas methods[8, 2, 14], which also achieve quantitative correctness. They are also related to coupled map lattices and discrete methods derived from them[1].

In section 2 we describe the construction of the new class of CAs and in section 3 we present the automaton using the Brandeisator model for the chlorite-iodide-malonic acid (CIMA) reaction as an example.

2 A New Cellular Automaton

The cellular automaton updates a regular lattice in discrete time steps. In this discretization of space and time the CA is not different from explicit finite difference methods for solving par-

tial differential equations (PDEs). Numerical PDE solvers usually use floating point arithmetic to solve the discretized equations. This use of floating point numbers implies some discretization, since the precision is limited (e.g. to 8 decimal digits). Usually it is assumed that the discretization error is negligible. In contrast to this floating point approach, we discretize all concentrations using only a small number of levels. This makes the new method a real cellular automaton. The main benefit of this strong discretization is the possibility of using a lookup table to replace the evaluation of the nonlinear rate functions. It is this use of a lookup table that accounts for a speedup of about one order of magnitude on a conventional workstation. The undesirable effects of discretization are overcome by using probabilistic rules for the updating of the CA.

The state of the CA is given by a regular array of concentration vectors $\mathbf{y}$ residing on a d-dimensional lattice. Each $\mathbf{y}(\mathbf{r})$ is a s-vector of integers (s is the number of reactive species). For reasons of efficiency, and to fulfill the finiteness condition of the definition of cellular automata, each component $\mathbf{y}_i(\mathbf{r})$ can only take integer values between 0 and $\mathbf{b}_i$, where the $\mathbf{b}_i$'s can be different for each species i. The position index $\mathbf{r}$ is a d-dimensional vector on the CA lattice. For cubic lattices, $\mathbf{r}$ is a d-vector of integers.

The central operation of the automaton consists of calculating the sum

$$\tilde{\mathbf{y}}_i(\mathbf{r}) = \sum_{\mathbf{r}' \in N_i} \mathbf{y}_i(\mathbf{r} + \mathbf{r}') \tag{1}$$

of the concentrations in some neighborhood N_i. The neighborhoods can be different for each species i. A neighborhood is specified as a set of displacement vectors. We use square neighborhoods in two dimensions, so that

$$N_i = \{(r_x, r_y) \,|\, r_x, r_y \text{ integer}, |r_x| \le r, |r_y| \le r\}\,, \tag{2}$$

which fulfils the necessary symmetry and isotropy requirements. For such neighborhoods, the summing operation can be executed in an extremely efficient way by using moving averages: in one dimension, the sum of all $2k+1$ cells centered around cell r can be computed from the corresponding sum centered around cell $r-1$ with just one addition and subtraction:

$$\begin{aligned} \tilde{\mathbf{y}}_i(r) &= \sum_{|r'| \le k} \mathbf{y}_i(r + r') \\ &= -\mathbf{y}_i(r-k-1) + \tilde{\mathbf{y}}_i(r-1) + \mathbf{y}_i(r+k). \end{aligned} \tag{3}$$

Using this relationship recursively, and using the fact that the sum over a square neighborhood in d dimensions can be constructed as the convolution of such one-dimensional sums applied in each dimension in turn, one obtains an algorithm to compute the sum of all cells in a square (cubic) neighborhood with only $2d$ additions per cell [15]. In a multispecies model several variables are necessary, but they can be packed into one computer word. In this case the averaging operation can be performed on several species at once if the diffusion coefficients are equal.

In the following we use the normalized values $\mathbf{x}_i(\mathbf{r}) = \mathbf{y}_i(\mathbf{r})/\mathbf{b}_i$ and $\tilde{\mathbf{x}}_i(\mathbf{r}) = \tilde{\mathbf{y}}_i(\mathbf{r})/(\mathbf{b}_i|N_i|)$, which are always between zero and one. The resulting fields $\tilde{\mathbf{x}}_i(\mathbf{r})$ are then the local averages of the $\mathbf{x}_i(\mathbf{r})$. *The averaging has the effect of diffusion.* This can be seen from a Taylor expansion of $\mathbf{x}_i(\mathbf{r} + \mathbf{r}')$ around $\mathbf{x}_i(\mathbf{r})$:

$$\begin{aligned} \tilde{\mathbf{x}}_i(\mathbf{r}) &= \frac{1}{|N_i|} \sum_{\mathbf{r}' \in N} \sum_{\kappa=0}^{\infty} \frac{1}{\kappa!} \left(\mathbf{r}' \frac{\partial}{\partial \mathbf{r}'} \right)^{\kappa} \mathbf{x}_i(\mathbf{r}) \\ &= \mathbf{x}_i(\mathbf{r}) + D_i \nabla^2 \mathbf{x}_i(\mathbf{r}) + \cdots \end{aligned} \tag{4}$$

The factors D_i can be computed as shown in [15] and are easily calculated from (4) for square neighborhoods with radius k: $D_i = k(k+1)/6$.

The second operation in the cellular automaton is the implementation of the reactive processes described by a rate law. Given the reaction-diffusion equation

$$\frac{\partial \mathbf{z}}{\partial t} = \mathbf{\Phi}(\mathbf{z}) + \mathcal{D}\nabla^2 \mathbf{z} \tag{5}$$

(where ∇^2 is understood to be a spatial operator acting on each component of the vector $\mathbf{z}$ separately, and $\mathcal{D}$ is a diagonal matrix), we discretize the time derivative to obtain

$$\mathbf{z}^{t^*+\Delta t} = \mathbf{z}^{t^*} + \Delta t \mathbf{\Phi}(\mathbf{z}^{t^*}) + \Delta t \mathcal{D}\nabla^2 \mathbf{z}^{t^*}. \tag{6}$$

Changing the time and space scales by setting $t = t^*/\Delta t$ and $r = r^*/\Delta r$, and using the variable $\mathbf{x}$ for the rescaled set gives

$$\mathbf{x}^{t+1} = \mathbf{x}^t + \Delta t \mathbf{\Phi}(\mathbf{x}^t) + \frac{\Delta t}{\Delta r^2}\mathcal{D}\nabla^2 \mathbf{x}^t. \tag{7}$$

as the equation to be treated by the CA. Let us define

$$\mathbf{\Phi}^*(\mathbf{x}) = \mathbf{x} + \Delta t \mathbf{\Phi}(\mathbf{x}). \tag{8}$$

From eqns. (4) and (8)

$$\begin{aligned} \mathbf{\Phi}^*(\tilde{\mathbf{x}}^t) &= \mathbf{x}^t + D_i\nabla^2\mathbf{x}^t + \cdots + \Delta t \mathbf{\Phi}(\mathbf{x}^t + D_i\nabla^2\mathbf{x}^t + \cdots) \\ &= \mathbf{x}^t + D_i\nabla^2\mathbf{x}^t + \Delta t \mathbf{\Phi}(\mathbf{x}^t) + \mathrm{O}(\Delta t^2). \end{aligned} \tag{9}$$

Then

$$\mathbf{x}^{t+1} = \mathbf{\Phi}^*(\tilde{\mathbf{x}}^t) \tag{10}$$

is consistently first order accurate in time and within this limit, eq. (10) can be validly identified with eq. (7) to describe the evolution of the system. The identification yields

$$D_i = \frac{\Delta t}{\Delta r^2}\mathcal{D}_i \qquad (\ i = 1, \cdots, s) \tag{11}$$

which defines the space scale. As $\tilde{\mathbf{y}}$ is the result of the diffusion step, the average output of the CA reaction-diffusion process should therefore be given by

$$\mathbf{g}_j = \mathbf{b}_j \mathbf{\Phi}^* \left(\left\{ \frac{\tilde{\mathbf{y}}_i}{\mathbf{b}_i |N_i|} \right\}_{i=1}^{s} \right) \tag{12}$$

for species j. [1]

A deterministic discretization of the rate law, as it is used in some discrete coupled map methods [1], may produce problems: due to the discretization spurious steady states or oscillations can appear. It is at this stage that the probabilistic rules come into effect. Given an input configuration $\tilde{\mathbf{y}}^t(\mathbf{r})$, one assigns new values $\mathbf{y}^{t+1}(\mathbf{r})$ probabilistically in such a way that the *average* result corresponds to the finite difference approximation to the given reaction-diffusion equation, $\mathbf{g}_i$. The simplest CA rule for the reactive step is to treat each species separately and use $\mathbf{y}_j^{t+1} = \lfloor \mathbf{g}_j \rfloor + 1$ with probability ($\mathbf{g}_j$ mod 1) and $\mathbf{y}_j^{t+1} = \lfloor \mathbf{g}_j \rfloor$ otherwise ($\lfloor e \rfloor$ is the largest integer smaller than or equal to e). In this way the average is exactly $\mathbf{g}_j$. Clearly this method introduces the minimal amount of noise for a given set of $\mathbf{b}_i$'s. In case higher noise levels are desired (e.g., if one wants to evaluate the role of fluctuations [14]), one can choose a different set of output values and associated probabilities with the same average $\mathbf{g}_j$, but different variance. To do so, in general at least three different possible outcomes (e.g. $\lfloor \mathbf{g}_j \rfloor - 1$, $\lfloor \mathbf{g}_j \rfloor$, $\lfloor \mathbf{g}_j \rfloor + 1$) are necessary.

[1] Possibly the function $\mathbf{\Phi}^*$ needs to be truncated to conform to the condition $\mathbf{\Phi}^* \in [0,1]^s$.

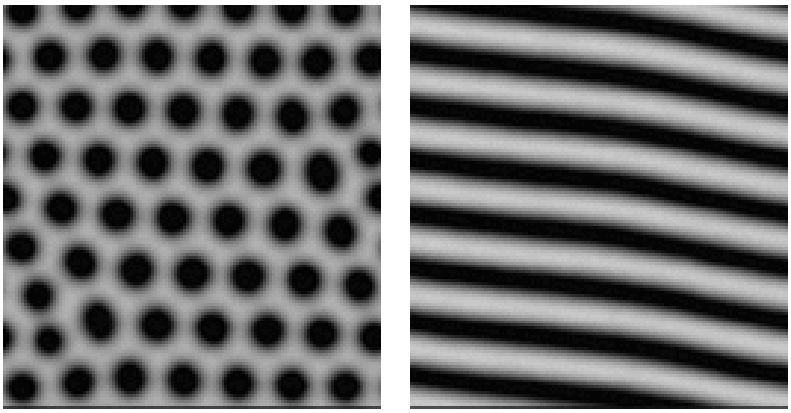

Figure 1: Regular spatial patterns that appear in the CIMA model, Eqs. (13) and (14): hexagons ($B = 20$) and stripes ($B = 13$). System size is 128^2 cells, and the boundary conditions are periodic.

3 The new CA applied to the Brandeisator (CIMA-model)

We will demonstrate the new CA using a simple model [9] for the CIMA (chloride-iodide-malonic acid) reaction, in which Turing patterns were first observed in the laboratory[11, 3]. The reaction-diffusion equations are

$$\dot{u} = D_u \nabla^2 u + A - u - \frac{uv}{1+u^2} \tag{13}$$

$$\dot{v} = D_v \nabla^2 v + 4Bu - B\frac{uv}{1+u^2}. \tag{14}$$

This model allows Turing patterns for some parameter values as long as $D_v > D_u$. We use $D_v = 10D_u$, which is within the experimental range. For values of $A > 6.455$ and small values of B, the system oscillates. For intermediate values of B, Turing structures appear, and for large values of B, the steady state is stable. Examples of patterns are shown in Fig. 1. The interesting fact is that both the Hopf bifurcation (for the appearance of oscillations) and the Turing bifurcation are subcritical for the parameter value $A = 30$ which we use here. This means that oscillations and patterns can coexist, and that patterns can coexist with uniform stable regions[6].

To study the different behaviors, we first start with a uniform system at the steady state and traverse the interesting range of values B in both directions. This simulation is performed with $\mathbf{b}_u = 56$ levels and averaging radius $r_u = 1$ for variable u, and $\mathbf{b}_v = 25$ levels and averaging radius $r_v = 4$ for variable v. We use a time step of $\Delta t = 0.03$. Figure 2 shows the bifurcation diagram which was obtained by simulating for at least 3 time units between each change of the parameter to reach the steady state. The different nonuniform structures that appear are shown in Figure 1. The system exhibits the following behaviors: The uniform steady state is stable for $B \geq 26$. Hexagons are stable between $B = 15$ and $B = 46$. Between $B = 7$ and $B = 32$, stripes are stable. For $7 \leq B \leq 11$, these stripes are not stationary, but oscillate ("ring"). The amplitudes given in Figure 2 for the nonuniform structures are only indications, since they depend strongly on the presence of defects (which we eliminated here), and the particular discrete wavenumber selected by the initial conditions. For $B \leq 20$, homogeneous oscillations are stable. Note that there are overlaps between the ranges of stability of different types of behaviors.

The overlap between oscillations and stripes leads to a special situation when a phase singularity of the oscillation is included in the simulation domain. Such a phase singularity can

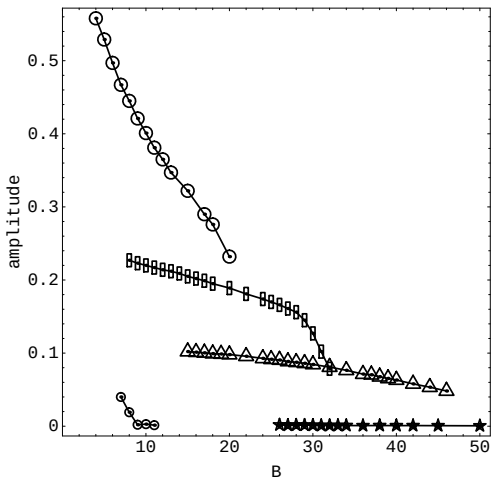

Figure 2: Bifurcation diagram for $A = 30$ indicating the magnitude of the largest space- or time-Fourier component for the variable u. Stars are used for the spatial component for uniform non-oscillating systems. Triangles are used for hexagonal patterns, and rectangles for striped patterns. The large circles indicate the amplitude of the limit cycle (averaged over the whole system), while the small circles indicate the amplitude of the oscillations of stripes.

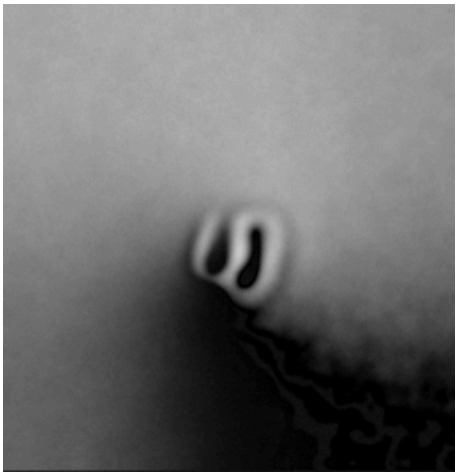

Figure 3: Oscillating spiral (only the tip is visible) with two spots in the center at $B = 15$. The rapidly rotating spiral makes the spots rotate slowly, too. System size is 256^2.

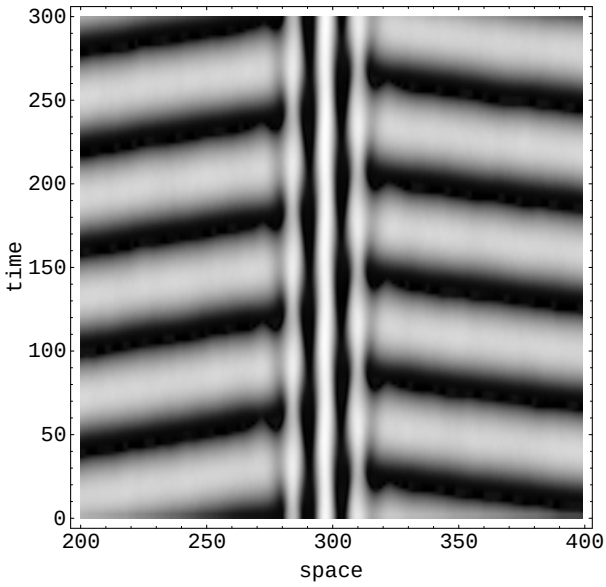

Figure 4: Space-time diagram of stripes surrounded by oscillations at $B = 15$.

only disappear by merging with another phase singularity (or the boundary), and leads to the formation of an oscillating spiral. At the phase singularity the conditions are similar to the steady state, which is unstable in this case, and lead to the formation of one or more spots (stripes for smaller B), as shown in Figure 3.

In the same parameter range (here $B = 15$), in a system with large aspect ratio (here $600 * 12$), stripes form easily. We now induce oscillations on both sides of the system. These oscillations coexist with stripes, and even with one single stripe, if the oscillations on both sides of the stripe are in opposite phase. A space-time diagram of this situation is shown in Figure 4. A similar situation was observed experimentally [12]. The difference between the experimental observations and this simulation is that here the oscillations form waves that move towards the stripes, whereas in the experiment the spot in the middle seemed to emanate waves. The direction of the wave propagation is determined by the influence of the stationary structures on the oscillation frequency in the neighborhood. In our simulation, the stripes seem to reduce the frequency, while in the experiment, the stable structure in the center increased the frequency. Comparing the frequency of oscillation ("ringing") of stripes at $B = 11$, which is approximately $\omega = 0.072$, with the frequency of homogeneous oscillations at the same parameter value, $\omega = 0.0866$, confirms that the stripes oscillate at a lower frequency and should therefore act as a sink of waves.

The overlap between hexagons and uniform steady state makes it possible to have groups of hexagons surrounded by the uniform steady state. This is illustrated in Figure 5

The overlap between hexagons and stripes implies that patterns of stripes and hexagons can be stable. The evolution of such patterns is mediated by the defects that exist in either structure, and the evolution is extremely slow.

4 Conclusion

We have constructed a class of cellular automata that can be used to model many reaction-diffusion systems with quantitatively correct results. The solutions are very isotropic despite

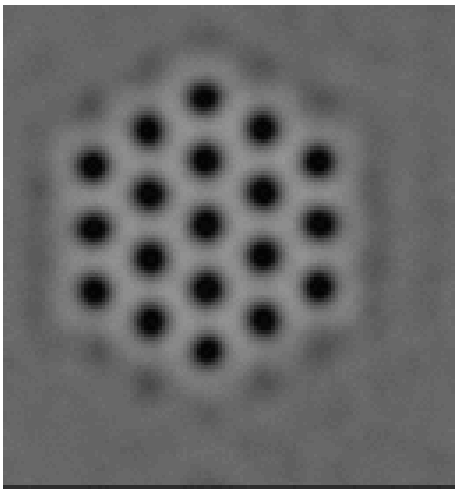

Figure 5: Hexagons surrounded by steady state at $B = 35$.

the discreteness and the anisotropic nature of the CA. The adverse effects of discretization are overcome by the use of probabilistic rules. In this respect the new CAs are similar to reactive lattice gas methods[8, 2, 14]. The main improvement is that the noise level is very much reduced by using a large number of states per cell. Due to this reduced noise level the new CA is much more efficient for the simulation of macroscopic phenomena than the lattice gas methods. In lattice gas methods both the reaction step and the diffusion (propagation) step introduce noise, which leads to fluctuations. These fluctuations are being studied in their own right and have been shown to exhibit some desirable properties [14], but in the simulation of macroscopic phenomena a high noise level is mostly undesirable. The new CA method achieves a reduction of the noise level for the reactive step and does not introduce noise in the diffusive step.

We have demonstrated the applicability of the automaton by investigating the Brandeisator model. We obtain oscillations, Turing patterns in the form of stripes and hexagons, and stability of the steady state. We find that the ranges of stability of most of these solutions overlap. We demonstrate the effect of these overlaps by showing some of the coexistences that are possible.

We acknowledge support from the European Community (SC1-0212), Fonds National de la Recherche Scientifique (JPB), Gottlieb Daimler- und Karl Benz-Stiftung (JRW) and Stiftung Stipendien-Fonds des Verbandes der Chemischen Industrie (JRW).

References

[1] Merk-Na Chee, Raymond Kapral, and Stuart G. Whittington. Phase resetting dynamics for a discrete reaction-diffusion model. *J. Chem Phys*, 92(12):7315–7322, 1990.

[2] David Dab, Jean-Pierre Boon, and Yue-Xian Li. Lattice-gas automata for coupled reaction-diffusion equations. *Phys. Rev. Lett.*, 66(19):2535–2538, 1991.

[3] P. de Kepper, V. Castets, E. Dulos, and J. Boissonade. Turing-type chemical patterns in the chlorite-iodide-malonic acid reaction. *Physica D*, 49:161–169, 1991.

[4] Martin Gerhardt, Heike Schuster, and John J. Tyson. A cellular automaton model of excitable media including curvature and dispersion. *Science*, 247:1563–1566, 1990.

[5] J. M. Greenberg and S. P. Hastings. Spatial patterns for discrete models of diffusion in excitable media. *SIAM J. Appl. Math.*, 34(3):515–523, 1978.

[6] Ole Jensen, Viggo O. Pannbacker, Guy Dewel, and Pierre Borckmans. Subcritical transitions to turing structures. *Phys. Lett. A*, 179:91–96, 1993.

[7] Raymond Kapral. Discrete models for chemically reacting systems. *J. of Mathematical Chemistry*, 6:113–163, 1991.

[8] Anna Lawniczak, David Dab, Raymond Kapral, and Jean-Pierre Boon. Reactive lattice gas automata. *Physica D*, 47:132–158, 1991.

[9] Istvàn Lengyel and Irving R. Epstein. Modeling of turing structures in the chlorite-iodide-malonic acid-starch reaction system. *Science*, 251:650–652, 1991.

[10] Mario Markus and Benno Hess. Isotropic cellular automaton for modeling excitable media. *Nature*, 347:56–58, 1990.

[11] Q. Ouyang and Harry L. Swinney. Transition from a uniform state to hexagonal and striped turing patterns. *Nature*, 352:610–612, 1991.

[12] J.-J. Perraud, A. De Wit, E. Dulos, P. De Kepper, G. Dewel, and P. Borckmans. One-dimensional "spirals": Novel asynchronous chemical wave sources. *Phys. Rev. Lett.*, 71(8):1272–1275, 1993.

[13] Hans E. Schepers and Mario Markus. Two types of performance of an isotropic cellular automaton: stationary (turing) patterns and spiral waves. *Physica A*, 188:337–343, 1992.

[14] Jörg R. Weimar, David Dab, Jean-Pierre Boon, and Sauro Succi. Fluctuation correlations in reaction-diffusion systems: Reactive lattice gas automata approach. *Europhysics Letters*, 20(7):627–632, 1992.

[15] Jörg R. Weimar, John J. Tyson, and Layne T. Watson. Diffusion and wave propagation in cellular automaton models of excitable media. *Physica D*, 55:309–327, 1992.

[16] Jörg R. Weimar, John J. Tyson, and Layne T. Watson. Third generation cellular automaton for modeling excitable media. *Physica D*, 55:328–339, 1992.

[17] Stephen Wolfram, editor. *Theory and applications of cellular automata; including selected papers '83-'86*, volume 1 of *Advanced Series on Complex Systems*. World Scientific, Singapore, 1986.